Structural Evolution in Mechanically Alloyed Al-Fe Powders

D.K. MUKHOPADHYAY, C. SURYANARAYANA, and F.H. (SAM) FROES

The structural evolution in mechanically alloyed binary aluminum-iron powder mixtures containing 1, 4, 7.3, 10.7, and 25 at. pct Fe was investigated using X-ray diffraction (XRD) and electron microscopic techniques. The constitution (number and identity of phases present), microstructure (crystal size, particle size), and transformation behavior of the powders on annealing were studied. The solid solubility of Fe in Al has been extended up to at least 4.5 at. pct, which is close to that observed using rapid solidification (RS) (4.4 at. pct), compared with the equilibrium value of 0.025 at. pct Fe at room temperature. Nanometer-sized grains were observed in as-milled crystalline powders in all compositions. Increasing the ball-to-powder weight ratio (BPR) resulted in a faster rate of decrease of crystal size. A fully amorphous phase was obtained in the Al-25 at. pct Fe composition, and a mixed amorphous phase plus solid solution of Fe in Al was developed in the Al-10.7 at. pct Fe alloy, agreeing well with the predictions made using the semiempirical Miedema model. Heat treatment of the mechanically alloyed powders containing the supersaturated solid solution or the amorphous phase resulted in the formation of the Al_3Fe intermetallic in all but the Al-25 at. pct Fe powders. In the Al-25 at. pct Fe powder, formation of nanocrystalline Al_5Fe_2 was observed directly by milling. Electron microscope studies of the shock-consolidated mechanically alloyed Al-10.7 and 25 at. pct Fe powders indicated that nanometer-sized grains were retained after compaction.

I. INTRODUCTION

A number of "far from equilibrium" synthesis techniques have been developed during the past few years to produce materials with improved properties; these include rapid solidification (RS) processing, vapor deposition, and mechanical alloying (MA).[1,2] Even though the principles utilized in these various processing techniques are quite different, the main objective of all of them is the same—improved microstructural and constitutional flexibility/control, thereby allowing enhanced physical and mechanical properties. Mechanical alloying is a solid-state powder processing technique that involves repeated welding, fracturing, and rewelding of powder particles in a dry, high-energy ball mill.[3,4,5] Mechanical alloying has been shown to be a powerful technique in allowing even further excursions from equilibrium than RS,[2] in addition to its more traditional application of producing oxide-dispersion–strengthened (ODS) nickel- and iron-base alloys.[3,4] The presence of these nonequilibrium phases allows greater flexibility and control of the final equilibrium microstructure, thereby producing materials with properties superior to those obtained by more conventional ingot metallurgy and casting techniques. The nonequilibrium phases synthesized by MA include supersaturated solid solutions, metastable crystalline or quasicrystalline intermediate (intermetallic) phases, and amorphous phases.[4,6] Mechanical alloying also results in a highly refined microstructure with a grain size down to nanometer levels.[7,8]

D.K. MUKHOPADHYAY, Graduate Student, Department of Metallurgical and Mining Engineering, is with the University of Idaho. C. SURYANARAYANA, Professor, Department of Metallurgical and Mining Engineering, and Associate Director, Institute for Materials and Advanced Processes, and F.H. FROES, Professor, Department of Metallurgical and Mining Engineering, and Director, Institute for Materials and Advanced Processes, are with the University of Idaho, Moscow, ID 83844-3026.

Manuscript submitted August 22, 1994.

Alloying of Al with Fe increases the high-temperature strength due to a dispersion of second-phase particles,[9] an effect that can be enhanced by increasing the volume fraction of the second phase after increasing the solid solubility extension of Fe in Al by techniques such as RS[9] or MA.[10] The Al-Fe phase diagram is shown in Figure 1 and the equilibrium solid solubility of Fe in Al at room temperature has been reported to be 0.025 at. pct.[11]*

*All compositions in this article are expressed in at. pct unless otherwise mentioned.

Intermetallic compounds generally have very high melting points and therefore can potentially be used for high-temperature structural applications, but they are brittle at room temperature. It has been shown that nanostructured materials have improved ductility over their coarse-grained counterparts.[12] Generally, synthesis of intermetallics is not achieved directly by MA;[13] rather, a subsequent annealing is required. However, there are some reports of synthesis of intermetallic compounds directly by milling in the Al-Fe system.[14,15]

Amorphous phases possess an interesting combination of properties and provide several potential advantages (*e.g.*, high strength and good corrosion resistance).[16] The amorphous structure can also be used as a precursor to synthesize nanostructured material, and the microstructure can be controlled as desired.[17]

The intent of this article is to report results of our extensive investigations on MA of Al-Fe alloys containing from 1 to 25 pct Fe and analyze the results of formation of nanostructures, intermetallic compounds, and metastable phases, including supersaturated solid solutions and amorphous phases. Mechanical alloying was earlier applied to the Al-Fe system to produce supersaturated solid solutions and amorphous phases in different alloy compositions.[14,18–22] The composition ranges for the formation of these phases are different depending on the severity of milling (type of mill) (Table I).

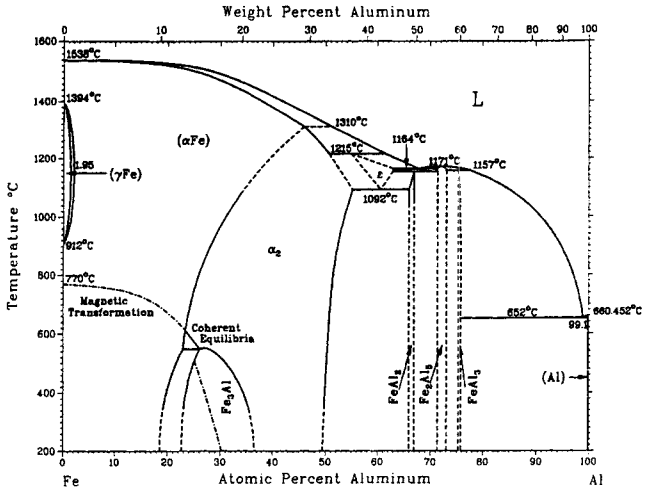

Fig. 1—Al-Fe equilibrium diagram.

II. EXPERIMENTAL PROCEDURE

Nominally pure Al (>99.4 pct and −100 mesh) and Fe (>99.4 pct and −325 mesh) powders were used as starting powders to make up mixtures containing 1, 4, 7.3, 10.7, and 25 pct Fe, with the last composition corresponding to stoichiometric Al_3Fe intermetallic. Mechanical alloying was carried out at room temperature in a SPEX* 8000 Mixer mill. The grinding medium was 4.75-mm-diameter hardened 52100 steel balls. For each run, approximately 10 g of powder mixture and 100 g of steel balls were used. The SPEX mill vial was cooled from outside during operation, using a fan to minimize the temperature rise of the powder inside the vial. Small quantities of the powder were withdrawn from the vials at regular time intervals inside an argon-filled glove box to follow the progress of alloying via X-ray diffraction (XRD), transmission electron microscopy (TEM), and scanning electron microscopy (SEM) techniques. The milled powders were heat-treated by sealing them in evacuated glass tubes to evaluate the stability of the phases formed. The mechanically alloyed powders were compacted by a shock consolidation method,[23] and the compacted specimens were also characterized by XRD, SEM, and TEM techniques.

*SPEX is a trademark of SPEX Industries, Edison, NJ.

III. RESULTS

A. *General Observations*

In all five alloys investigated (Al-1, 4, 7.3, 10.7, and 25 pct Fe), a decrease in the particle size was observed with increasing milling time. Figure 2 shows SEM micrographs of the Al-4 pct Fe powder in as-blended condition and after milling for 10 and 20 hours, indicating that the particle size decreases with increasing milling time. A similar situation was obtained in all the other compositions. A high-magnification SEM micrograph (Figure 3) shows that each of the powder particles is made up of fine grains, which have nanometer dimensions; <100 nm in size in the Al-10.7 pct Fe powder mechanically alloyed up to 30 hours.

The XRD patterns in each case showed that the Al(200) and Al(220) peaks overlap with Fe(110) and Fe(200) peaks, respectively; only the Al(111) and Al(311) peaks are seen clearly and separately. Increasing milling time caused the peaks to broaden and decrease in intensity as a result of both the refinement of crystal size and the introduction of strain during milling. In powders with high Fe contents, the Al(111) peak has a lower intensity than the Al(200) peak, whereas at lower Fe contents, the Al(111) peak is more intense, as expected. The Al crystal size was calculated for each condition from the broadening of X-ray peaks using the Scherrer formula[24] and subtracting the strain and instrumental broadening effects. Details of these calculations have been published elsewhere.[25] Nanometer-sized crystals are formed in all the alloys after long MA times (Figure 4). Increasing the ball-to-powder weight ratio (BPR) resulted in a faster rate of decrease of crystal size (Figure 5).

B. *Solid Solution Formation*

Figure 6 shows the XRD patterns of the Al-7.3 pct Fe powder as a function of milling time. In the starting powder mixture, all the expected peaks from both Al and Fe can be seen, with the Fe(110) and Fe(200) peaks overlapping with the Al(200) and Al(220) peaks, respectively. With increased milling time, the Al peaks shifted to higher angles, suggesting alloying of Fe with Al, leading to formation of a solid solution. The lattice parameter of the Al solid solution, calculated from the position of the Al(311) peak, had decreased at 20 hours from the initial value of 0.4050 nm in the as-blended state to 0.4015 nm for the Al-7.3 pct Fe powder and 0.4022 nm for the Al-4 pct Fe powder. The lattice parameter thereafter remained constant, indicating that the maximum solubility level had been reached. These lattice parameters in different powder compositions were used to calculate the solid solubility in each case, using the master plot of lattice parameter *vs* Fe content plotted from the published literature on rapidly solidified Al-Fe alloys[26–31] (Figure 7). From this plot, it is clear that a maximum of 4.5 pct Fe can be dissolved in Al in the solid state by MA.

C. *Synthesis of Intermetallics*

Figure 8 shows the XRD patterns of the as-milled Al-25 pct Fe powder. After 15 hours of milling, partial formation of Al_5Fe_2 compound was observed.[15] The JCPDS (Joint Committee on Powder Diffraction Standards) data suggested that this compound is Al_5Fe_2 with an orthorhombic structure and a = 0.767 nm, b = 0.64 nm, and c = 0.42 nm. Complete formation of the Al_5Fe_2 compound was observed after 30 hours of milling. The peaks are relatively broad because of the fine crystal size and the presence of strain in the powder. Upon annealing the powder milled for 30 hours at 625 °C for 324 hours, sharp XRD lines resulted (Figure 9), including a number with low intensities that were not apparent in the as-milled powder. However, there is no difference either in the structure or the lattice parameters of this Al_5Fe_2 phase between the as-milled and annealed conditions. In the other compositions, however, formation of the intermetallic phases was not observed directly by milling; instead, either a solid solution or an amorphous phase or a mixture of these two phases was obtained. The XRD pattern of the Al-10.7 pct powder milled for 50 hours and heat-treated at 625 °C for 3 hours (Figure 10) showed the presence of both Al and Al_3Fe. Similar heat treatment

Table I. Summary of Previous Results on Solid Solution and Amorphous Phase Formation in Mechanically Alloyed Al-Fe Powders

Composition Range of Powder (Pct Fe)	Maximum Solid Solubility (Pct Fe)	Amorphous Phase Formation Range (Pct Fe)	Type of Ball Mill	Reference
12.5 to 25	—	20	planetary	14
4 to 42	1	17 to 33	horizontal	18,19
3.5	3.5	—	—	20
10 to 60	—	20 to 50	SPEX	21
20	—	20	SPEX	22

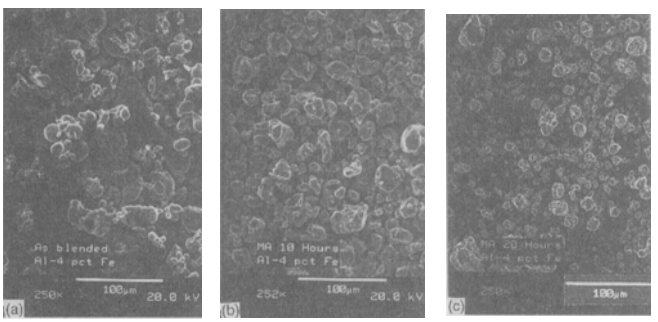

Fig. 2—Scanning electron micrographs of the Al-4 pct Fe powder (*a*) as-blended, (*b*) milled for 10 hours, and (c) milled for 20 hours, showing a decrease in the particle size with milling time.

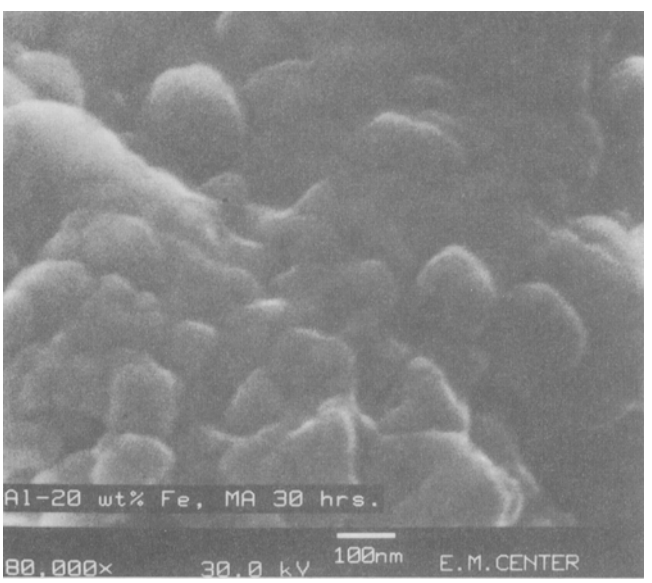

Fig. 3—Scanning electron micrograph of the Al-10.7 pct Fe powder mechanically alloyed for 30 hours, showing the presence of nanometer-sized crystals.

for the Al-4 pct Fe powder milled for 20 hours showed the formation of Al and Al_3Fe phases. The relative proportions of the Al and Al_3Fe phases obtained after heat treatment in these compositions were calculated using the integrated areas of the peaks of the different phases;[24] this matches well with that calculated from the equilibrium diagram.

D. *Amorphous Phase Formation*

As can be seen from the XRD pattern in Figure 8(e), a broad halo, suggestive of formation of an amorphous phase, was seen after milling the Al-25 pct Fe powder for 50 hours. Electron diffraction patterns confirm the formation of the amorphous phase in the powder (Figure 11). However, only partial amorphization was observed in the Al-10.7 pct Fe powder. Figure 12 shows an electron diffraction pattern from the Al-10.7 pct Fe powder showing the coexistence of the Al(Fe) solid solution and an amorphous phase even after milling for 50 hours. Amorphization was not observed in Al-1, 4, and 7.3 pct Fe compositions even after milling for long times (*e.g.*, 65 hours).

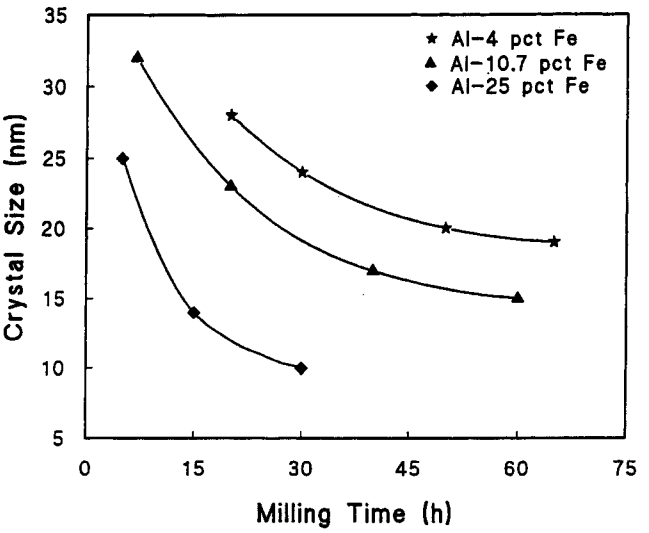

Fig. 4—Plot showing the variation of crystal size with milling time in Al-4, 10.7, and 25 pct Fe powders.

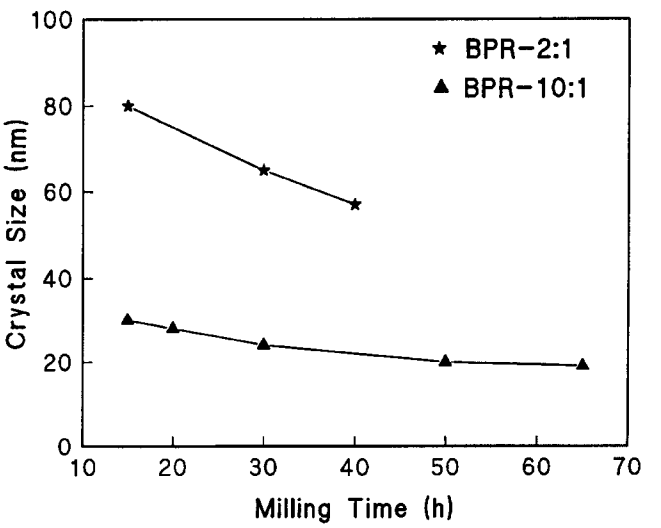

Fig. 5—Effect of BPR on the crystal size refinement by MA in Al-4 pct Fe powders.

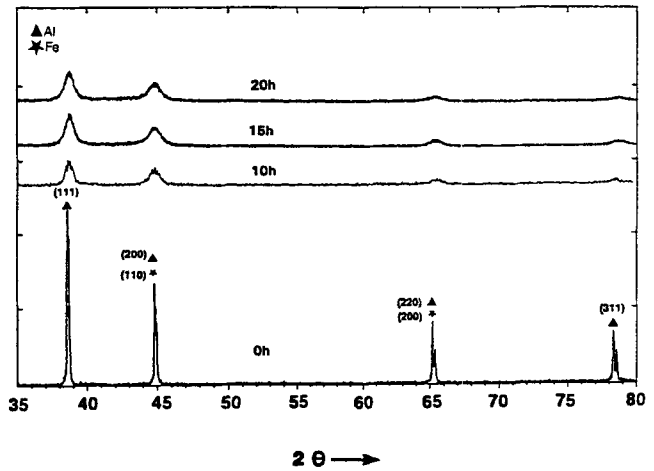

Fig. 6—X-ray diffraction patterns of Al-7.3 pct Fe powder as a function of MA time.

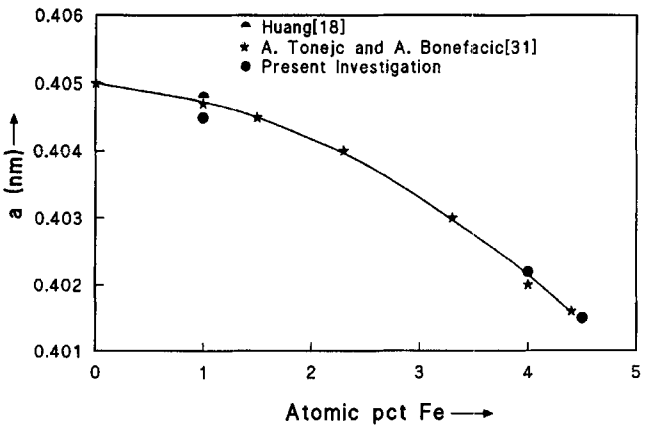

Fig. 7—Master plot showing the variation of lattice parameter of Al-solid solution with Fe content obtained by RS and MA techniques.

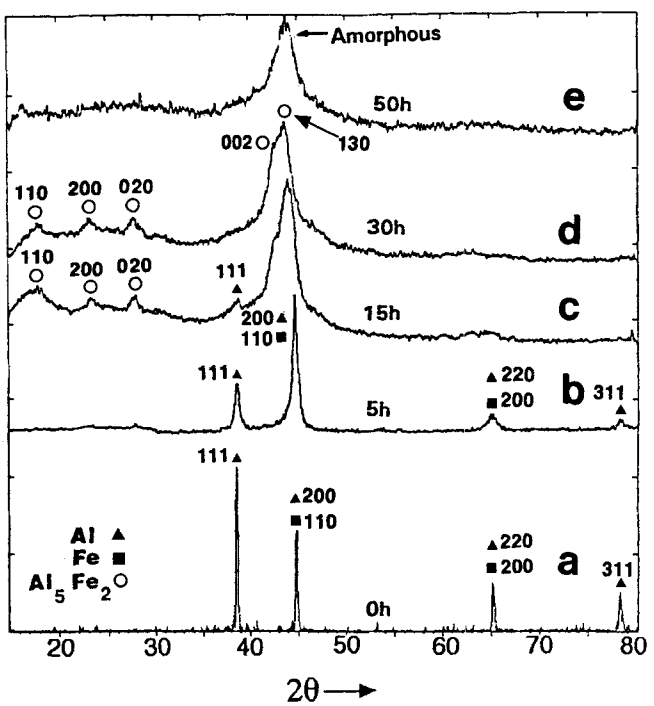

Fig. 8—X-ray diffraction patterns of Al-25 pct Fe powder as a function of MA time.

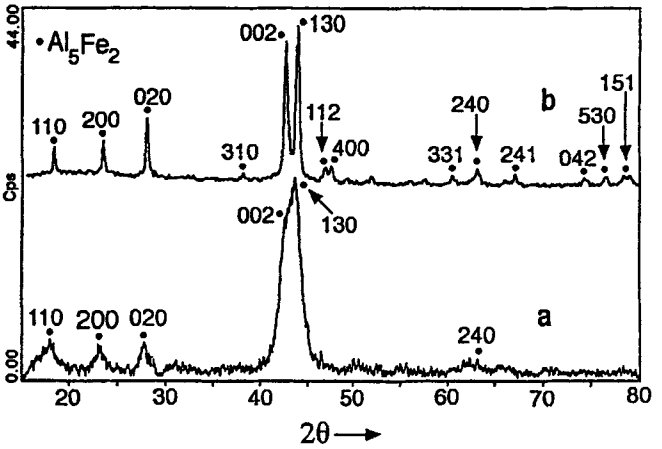

Fig. 9—X-ray diffraction patterns of the Al-25 pct Fe powders (a) mechanically alloyed for 30 hours and (*b*) mechanically alloyed for 30 hours and heat-treated at 625 °C for 324 hours.

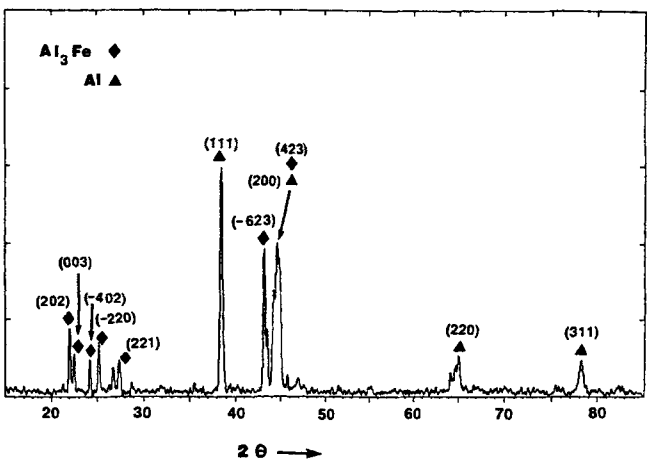

Fig. 10—X-ray diffraction pattern of the Al-10.7 pct Fe powder mechanically alloyed for 50 hours and subsequently annealed at 625 °C for 3 hours, showing the presence of Al and Al_3Fe phases.

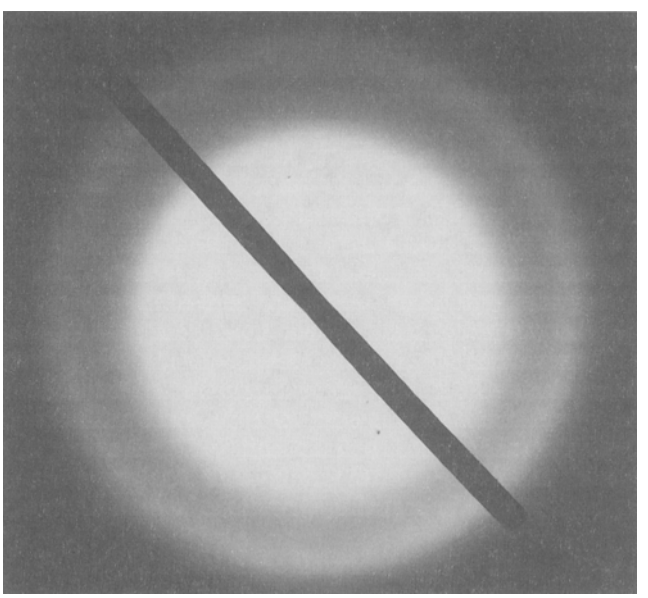

Fig. 11—Electron diffraction pattern of Al-25 pct Fe powder mechanically alloyed for 50 hours, showing full amorphization.

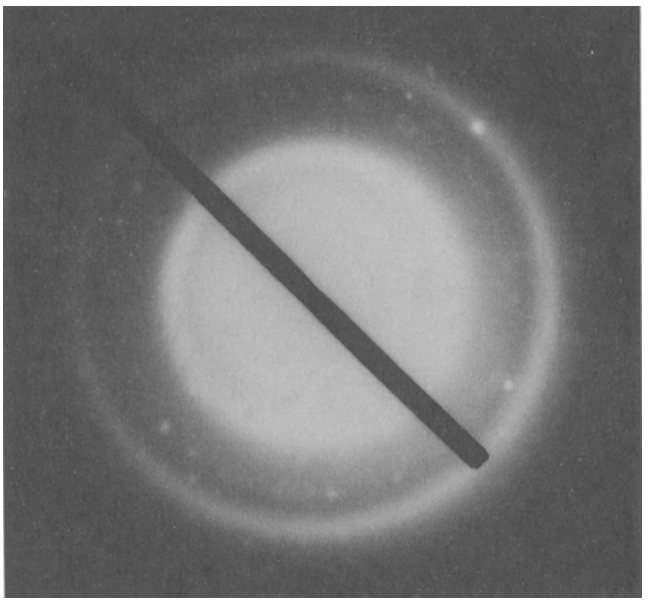

Fig. 12—Electron diffraction pattern of Al-10.7 pct Fe powder mechanically alloyed for 50 hours, showing partial amorphization.

E. *Consolidation*

The Al-10.7 pct and 25 pct Fe powders milled for 50 and 15 hours, respectively, were consolidated by shock compaction techniques to form dense pellets. Near 100 pct density was achieved in both the samples. X-ray diffraction patterns of the consolidated samples indicate the presence of the Al_3Fe and Al_5Fe_2 compounds in the 10.7 and 25 pct Fe powders, respectively, suggesting that decomposition of the solid solution has occurred. Transmission electron micrographs of the consolidated specimens (Figure 13) confirmed the retention of 25- to 30-nm grains, which indicates minimal grain growth during the shock consolidation.

A summary of the results of MA for different compositions is shown in Figure 14.

IV. DISCUSSION

Mechanical alloying of Al-Fe alloys has been shown to result in particle/grain size refinement, extension of the solid solubility limit of Fe in Al, and intermetallic compound and amorphous phase formation.

A. *General Observations*

With an increase in the milling time, broadening of the X-ray peaks was observed in all compositions. The broadening of the peaks is due to the fine crystal size and also due to the presence of strain in the powders. A comparison of the XRD patterns of Al-7.3 pct Fe and Al-25 pct Fe powders (Figures 6 and 8) shows that in the case of Al-7.3 pct Fe powder, the Al(111) peak is more intense than the Al(200)/Fe(110) peak even after 20 hours, and Al(220)/Fe(200) and Al(311) peaks are still present. But in the case of Al-10.7 pct and higher Fe contents, the Al(111) peak has a much lower intensity than the Al(200)/Fe(110) peak after long milling times. After continued milling, the Al(311) peak has completely disappeared, and the Al(220)/Fe(200) peak is very broad and has a low intensity. Similar results were reported earlier in the Al-Cr[32,33] and Al-Mo[34,35] systems after MA.

B. *Solid Solubility Extension*

The solid solubility limit of Fe in Al achieved in the present investigation is higher than that observed by Huang and co-workers,[18,19] probably a result of the higher energy SPEX mill used. Polkin *et al.*[20] observed a solid solubility of 3.5 pct Fe in Al by MA, but due to lack of any specific information (*e.g.*, type of mill, BPR) a detailed comparison of the work with our own is not possible. A number of investigators have reported solid solubility extension of Fe in Al by RS,[26–31] and these results are summarized in Table II along with those obtained by MA[18,19,20] and data from the present work. Table II shows that the solid solubility extension obtained in the Al-Fe system by MA is at least as high as the maximum extension observed using RS techniques.

Using RS techniques, large extensions of solid solubility limits are possible by quenching the alloy melts to below the T_0 temperature (the temperature at which the solid and liquid phases have the same free energy at a given composition),[36] and a metastable equilibrium is reached between the supersaturated solid solution and the intermetallic (if present in the system). Processing by the MA technique involves repeated welding and fracturing of the powder particles and results in a very intimate mixture of the two constituent powder particles with a concomitant increase in the defect concentration and strain in the powder mixture. Milling also refines the grain size. Since the diffusion distances are reduced, grain boundary area is increased. The defect density is high, enhancing diffusion rates so that true alloying occurs between the two constituents. However, in MA, a metastable equilibrium is reached between the supersaturated solid solution and the amorphous phase, and this limits the solid solubility.[37]

C. *Synthesis of Intermetallics*

In the Al-25 pct Fe powder mechanically alloyed for 15 hours, the Al_5Fe_2 intermetallic compound is produced directly by milling. Since the starting powder was of the overall Al_3Fe composition, energy-dispersive spectroscopy analysis was conducted on the mechanically alloyed powders to check whether the composition had changed upon MA. The analysis indicated that the powder contains 73.5 pct Al and 26.5 pct Fe. This change in composition can be due either to loss of Al due to sticking of the powder on the container wall and to the grinding balls, and/or due to a gain of Fe from the steel balls and container wall. Since the Al_5Fe_2 intermetallic forms under equilibrium conditions in the composition range of about 27 to 29 pct Fe,[11] it is not surprising that formation of homogeneous Al_5Fe_2 was observed in the present investigation at an Fe content of 26.5 pct. Similarly, Huang[18] observed the formation of the Al_5Fe_2 intermetallic in nominally Al-24.4 pct Fe powder heat-treated at 500 °C after MA for 180 hours.

To determine whether or not the Al_3Fe intermetallic can be synthesized directly by MA after compensating for the loss of Al, an extra amount of 1.5 pct Al was added to the nominal Al-25 pct Fe powder mix prior to MA. However, the Al_3Fe intermetallic phase did not form; instead, a solid

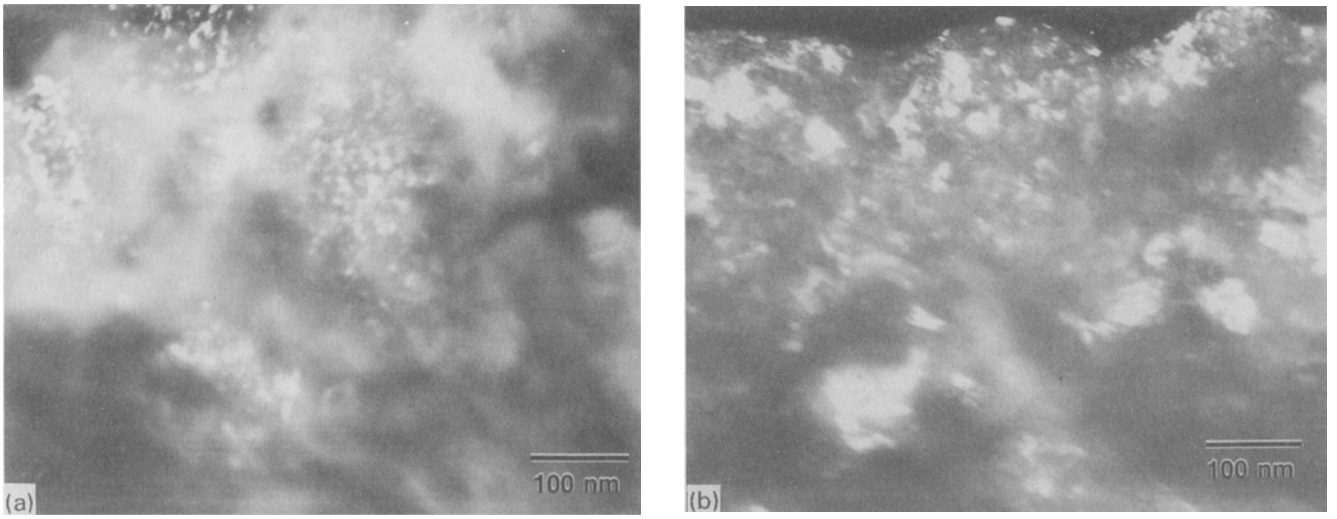

Fig. 13—Transmission electron micrographs of the shock-consolidated specimens of (*a*) Al-10.7 pct Fe powder mechanically alloyed for 65 hours and (*b*) Al-25 pct Fe powder mechanically alloyed for 15 hours, showing the presence of 25- to 30-nm nanocrystals.

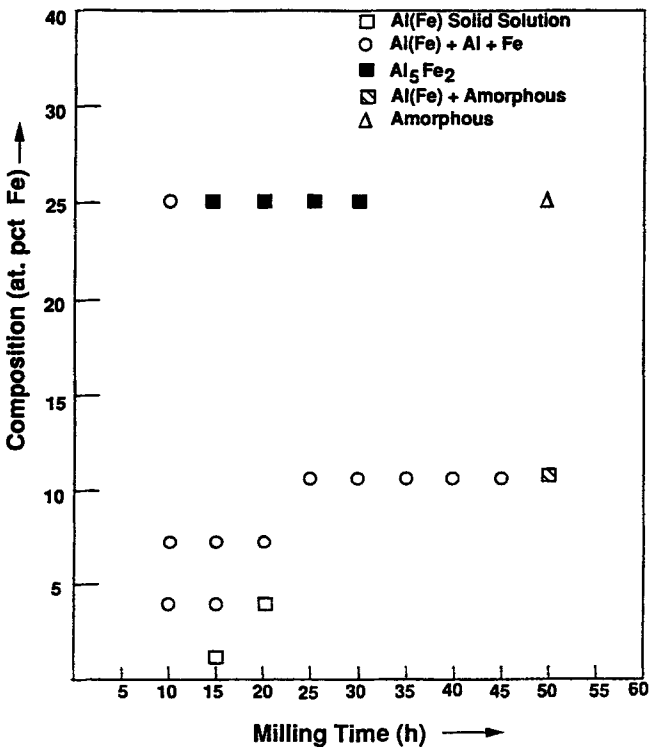

Fig. 14—A plot showing the phases formed at different compositions and milling times in Al-Fe powders.

Table II. Extension of Solid Solubility of Fe in Al by RS and MA Techniques

Equilibrium Solid Solubility (Pct Fe)	Extension by RS (Pct Fe)	Reference	Extension by MA (Pct Fe)	Reference
0.025	0.082	26	1	18,19
	3	27	3.5	20
	3.5	28	4.5	present
	3.7	29		work
	4	30		
	4.4	31		

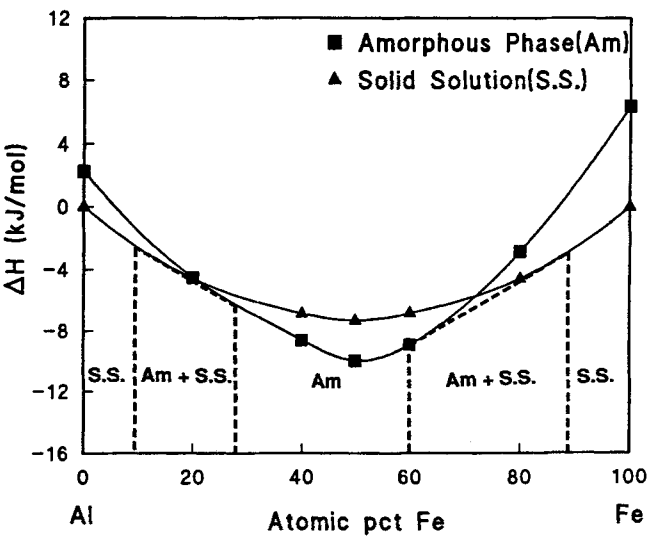

Fig. 15—Calculated enthalpy *vs* composition diagram for the Al-Fe system using the Miedema model.[38]

solution of Fe in Al formed at early milling times, and an amorphous phase formed after 50 hours. Although the enthalpy of formation of Al_3Fe (28.1 kJ/g-atom) is very close to that of Al_5Fe_2 (28.3 kJ/g-atom), Al_3Fe could not be directly synthesized, possibly as a result of the complex crystal (monoclinic) structure and large unit cell. The Miedema model[38] predicts that an amorphous phase should form in the composition range 25 to 60 pct Fe in the Al-Fe system, in agreement with the present work. The intermetallic Al_3Fe compound could only be synthesized in powders with lower Fe contents only after heat-treating the milled powders.

D. *Amorphous Phase Formation*

Miedema's semiempirical model[38] has been used to predict the glass-forming range in the Al-Fe system. The enthalpy *vs* composition diagram calculated using the Miedema model is shown in Figure 15. The common tangent construction suggests that a fully amorphous phase should form between 25 and 60 pct Fe. At compositions $x < 15$

Table III. Comparison of the Predicted Fully Amorphous Composition Range Calculated Using the Miedema Model with the Observed Range in the Al-Fe System

Predicted (Pct Fe)	Observed (Pct Fe)	Reference
25 to 60*	20**	14
	17 to 33	18
	20 to 50	21
	20**	22
	25†	present work

*According to the Miedema model.[38]
**Investigated only one composition.
†Partial amorphization was detected in the 10.7 pct Fe composition.

pct Fe and $x > 90$ pct Fe, only a solid solution is expected to be stable. In the intermediate ranges, 15 pct Fe $< x <$ 25 pct Fe and 60 pct Fe $< x <$ 90 pct Fe, both the amorphous phase and solid solution are predicted to coexist. Table III presents the composition ranges where a fully amorphous phase has been predicted by theory and obtained experimentally. This table shows that the predicted and observed composition ranges are very close according to Dong *et al.*,[21] but not for the data reported by Huang.[18] Morris and Morris[14] and Wang *et al.*[22] observed full amorphization in the Al-20 pct Fe composition, which is outside the composition range predicted by the Miedema model. In the present investigation, MA of Al-25 pct Fe showed full amorphization, which agrees with the prediction. In the Al-10.7 pct Fe composition, a mixture of an amorphous phase and a solid solution was observed that also matches well with the prediction of the Miedema analysis. However, the match of the model with the present work and with that of Dong *et al.*,[21] and the disagreement with the others, is not unexpected. The experimental parameters (type of ball mill, the BPR, the purity of the atmosphere during milling, *etc.*) are likely to influence the range over which the amorphous phase occurs. In fact, Koyano *et al.*[39] reported that an amorphous phase was obtained in ball-milled Fe-Cr alloy powders only in the presence of oxygen contamination; an intermetallic was reported to form in the absence of oxygen. Because of such differences in processing conditions, different investigators could obtain different results in the same alloy system. Thus, although it is recognized that the Miedema model[38] has limitations (*e.g.*, the model does not consider the presence of intermediate phases in the system), it is still the best available model at the present time to predict the glass-forming range.

V. CONCLUSIONS

Based on the results obtained on the MA of Al-Fe alloys with 1, 4, 7.3, 10.7, and 25 pct Fe, the following conclusions can be made.

1. Refinement of the crystal size to the nanometer dimensions was observed in all the compositions studied. Increasing the BPR resulted in a faster rate of decrease of crystal size.
2. A maximum extension of solid solubility of 4.5 pct Fe in Al was observed. The extension of solubility is at least as much as the maximum extension observed by the RS technique and can be rationalized on the basis of equilibrium between the supersaturated solid solution and the amorphous phase.
3. The Al_5Fe_2 intermetallic could be synthesized directly by MA in Al-25 pct Fe composition. The formation of intermetallic compound directly by MA was not observed in the other compositions (4, 7.3, and 10.7 pct Fe). Here, heat treatment of the milled powders was necessary to synthesize the intermetallic Al_3Fe compound.
4. A fully amorphous phase was observed in the Al-25 pct Fe powder after 50 hours of milling. A mixture of an amorphous phase and solid solution was observed in the Al-10.7 Fe composition. A thermodynamic analysis based on Miedema's model predicts that full amorphization should be observed in powders from 25 to 60 pct Fe; thus, the results of the present investigation concur with this prediction.
5. Shock consolidation of Al-10.7 and 25 pct Fe powders mechanically alloyed for 65 and 15 hours produced near 100 pct dense compacts. Transmission electron microscopy studies of the shock-consolidated material showed retention of nanometer-sized grains of 25 to 30 nm in both the Al-10.7 and 25 pct Fe powder compacts.

ACKNOWLEDGMENTS

The authors would like to acknowledge the help of Dr. Gary Korth of INEL for shock consolidating the milled powders. Part of the work reported here was supported by the U.S. Bureau of Mines under Contract No. JO 134035 through the Department of Energy Idaho Field Office Contract No. DE-AC07-76IDO1570, Dr. S. Dillich, program manager.

REFERENCES

1. P.H. Shingu: in *First Int. Conf. on Processing Materials for Properties*, H. Henein and T. Oki, eds. TMS, Warrendale, PA, 1993, pp. 1275-80.
2. F.H. Froes, C. Suryanarayana, K. Russell, and C.G. Li: *Int. J. Mechanochem. Mech. Alloying*, 1994, vol. 1, pp. 112-24.
3. J.S. Benjamin: *Metall. Trans.*, 1970, vol. 1, pp. 2943-51.
4. C.C. Koch: in *Processing of Metals and Alloys*, R.W. Cahn, ed., VCH Verlagsgesellschaft, Weinheim, F.R. Germany, 1991, Materials Science and Engineering—A Comprehensive Treatment, pp. 193-245.
5. D. Maurice and T.H. Courtney: *Metall. Trans. A.*, 1990, vol. 21A, pp. 289-303.
6. C. Suryanarayana and F.H. Froes: *Mater. Sci. Forum*, 1992, vol. 88-90, pp. 445-52.
7. C. Suryanarayana and F.H. Froes: *Metall. Trans. A.*, 1992, vol. 23A, pp. 1071-81.
8. C.C. Koch: *Nanostructured Mater.*, 1993, vol. 2, pp. 109-29.
9. *Dispersion Strengthened Aluminum Alloys*, Y.W. Kim and W.M. Griffith, eds., TMS, Warrendale, PA, 1988.
10. *Mechanical Alloying for Structural Applications*, J.J. deBarbadillo, F.H. Froes, and R. Schwarz, eds., ASM INTERNATIONAL, Materials Park, OH, 1993.
11. T.B. Massalski: *Binary Alloy Phase Diagrams*, ASM, Metals Park, OH, 1986, vol. 1, pp. 147-49.
12. C. Suryanarayana: *Bull. Mater. Sci.*, 1994, vol. 17, pp. 307-46.
13. C. Suryanarayana, F.H. Froes, D.K. Mukhopadhyay, G. Cizmich, G.H. Chen, Z. Peng, and J. Mishurda: in *Processing and Fabrication of Advanced Materials III*, V.A. Ravi, T.S. Srivatsan, and J.J. Moore, eds., TMS, Warrendale, PA, 1994, pp. 567-84.
14. M.A. Morris and D.G. Morris: *Mater. Sci. Eng. A*, 1991, vol. 136, pp. 59-70.
15. D.K. Mukhopadhyay, C. Suryanarayana, and F.H. Froes: *Scripta Metall. Mater.*, 1994, vol. 31, pp. 333-38.

16. *Metallic Glasses*, T.R. Anantharaman, ed., Trans Tech Pub., Aedermannsdorf, Switzerland, 1984.
17. C. Suryanarayana and F.H. Froes: *Nanostructured Mater.*, 1993, vol. 3, pp. 147-53.
18. B. Huang: Ph.D. Thesis, Kyoto University, Japan, 1990.
19. B. Huang, N. Tokijane, K.N. Ishihara, P.H. Shingu, and S. Nasu: *J. Non-Cryst. Solids*, 1990, vol. 117/118, pp. 688-91.
20. I.S. Polkin, E.J. Kaputkin, and A.B. Borzov: in *Structural Applications of Mechanical Alloying*, F.H. Froes and J.J. deBarbadillo, eds., ASM INTERNATIONAL, Materials Park, OH, 1990, pp. 251-56.
21. Y. Dong, W.H. Wang, L. Lin, K.Q. Xiao, S.H. Tong, and Y.Z. He: *Mater Sci. Eng. A*, 1991, vol. 134, pp. 867-71.
22. G. Wang, D. Zhang, H. Chen, B. Lin, W. Wang, and Y. Dong: *Phys. Lett. A*, 1991, vol. 155, pp. 57-61.
23. G. Korth: in *Advanced Synthesis of Engineered Structural Materials*, J.J. Moore, E.J. Lavernia, and F.H. Froes, eds., ASM INTERNATIONAL, Materials Park, OH, 1993, pp. 81-86.
24. B.D. Cullity: *Elements of X-Ray Diffraction*, Addison-Wesley Pub. Co., Reading, MA, 1976.
25. S.K. Pradhan, T. Chakraborty, S.P. Sengupta, C. Suryanarayana, A. Frefer, and F.H. Froes: *Nanostructured Mater.*, 1995, vol. 5, pp. 53-61.
26. G. Falkenhagen and W. Hofmann: *Z. Metallkd.*, 1952, vol. 43, p. 69.
27. A. Fontaine and A. Guinier: *Phil. Mag.*, 1971, vol. 31, p. 70.
28. M. De Sanctis, A.P. Woodfield, and M.H. Loretto: *Int. J. Rapid Solidification*, 1988, vol. 4, pp. 53-74.
29. A. Kamio, H. Tezuka, T. Sato, T.T. Long, and T. Takahashi: *J. Jpn. Inst. Light Met.*, 1986, vol. 36, pp. 72-80.
30. P. Furrer and H. Warlimont: *Z. Metallkd.*, 1973, vol. 64, pp. 236-48.
31. A. Tonejc and A. Bonefacic: *J. Appl. Phys.*, 1968, vol. 40, pp. 419-20.
32. K.F. Kobayashi, N. Tachibana, and P.H. Shingu: *J. Mater. Sci.*, 1990, vol. 25, pp. 801-04.
33. K.F. Kobayashi, N. Tachibana, and P.H. Shingu: *J. Mater. Sci.*, 1990, vol. 25, pp. 3149-54.
34. M.D. Zdujic, K.F. Kobayashi, and P.H. Shingu: *J. Mater. Sci.*, 1991, vol. 26, pp. 5502-08.
35. M.D. Zdujic, K.F. Kobayashi, and P.H. Shingu: *Z. Metallkd.*, 1990, vol. 81, pp. 380-85.
36. H. Jones: *Rapid Solidification of Metals and Alloys*, Institution of Metallurgists, London, 1982.
37. R.B. Schwarz, R.R. Petrich, and C.K. Saw: *J. Non-Cryst. Solids*, 1985, vol. 76, pp. 281-302.
38. A.K. Niessen, F.R. de Boer, R. Boom, P.F. de Chatel, W.C.M. Mattens, and A.R. Miedema: *CALPHAD*, 1983, vol. 7, pp. 51-70.
39. T. Koyano, T. Takizawa, T. Fukunaga, U. Mizutani, S. Kamizuru, E. Kita, and A. Tasaki: *J. Appl. Phys.*, 1993, vol. 73, pp. 429-33.